the benzene ring F. Intramolecular short contacts between the D and F rings, whose distances are smaller than 3·8 Å are shown in Fig. 2(b).

The projections of the crystal structure along the a and c axes are shown in Figs. 5 and 6, respectively. The molecules are designated by the molecular numbers I to IV as follows.:

I at (x, y, z),
II at $(\frac{1}{2}+x, -\frac{1}{2}+y, -z)$,
III at $(\frac{1}{2}-x, 1-y, \frac{1}{2}+z)$,
IV at $(1-x, \frac{1}{2}+y, \frac{1}{2}-z)$.

The x, y and z coordinates are as given in Table 1. The subscript attached to the molecular number in the Figures indicates translations along the three edges of the unit cell. The shortest intermolecular distances less than 3·8 Å are shown in these Figures. There are no abnormal distances between the molecules. One of the remarkable features of the packing of the molecules is the arrangement of the *p*-bromobenzenesulphonyl groups. As seen in Fig. 5, these groups are arranged head to tail along the c axis. The bromine atom lies on top of the sulphonyl group of the neighbouring molecule and at the same time close contacts between C(3) and the phenyl group (ring E) are produced. In this way, trains of the molecules are formed extending along the c axis. The shortest distance between the bromine atom and the sulphonyl oxygen atoms is 3·35 Å

[Br...O(4)] which corresponds to the sum of the van der Waals radii but a dipole interaction is expected for this arrangement. Fig. 6 shows the packing of the molecular trains. The shortest distance between the trains is found between the atoms O(5) of the sulphonyl oxygen atom and C(24) of the benzene ring. This distance, 3·14 Å is nearly the minimum van der Waals distance expected for this kind of contact.

References

BUSING, W. R., MARTIN, K. O. & LEVY, H. A. (1962). *ORFLS.* Oak Ridge National Laboratory, Oak Ridge, Tennessee, USA.

DAUBEN, C. H. & TEMPLETON, D. H. (1955). *Acta Cryst.* 8, 841.

HIRAI, K., NOZOE, S., TSUDA, K. & IITAKA, Y. (1967). *Tetrahedron Letters,* 2177.

International Tables for X-ray Crystallography (1962). Vol. III. Birmingham: Kynoch Press.

ISHIBASHI, K. (1962). *J. Antibiotics,* Ser. A, 15, 161.

OKAYA, Y. & ASHIDA, T. (1967). *HBLS* IV, *The Universal Crystallographic Computing System* (I), p. 65. Japanese Crystallographic Association.

Neutron Diffraction Study of Ba(N3)2

BY CHANG S. CHOI*

Explosives Laboratory, FRL, Picatinny Arsenal, Dover, New Jersey, U.S.A.

The crystal structure of anhydrous barium azide, $Ba(N_3)_2$, has been determined by single-crystal neutron diffraction methods. The unit cell is monoclinic, $a=9·59$, $b=4·39$, $c=5·42$ Å, $\beta=99·75°$; space group $P2_1/m$, with two molecules per cell. All atoms were shown by a Patterson map to lie on mirror planes. The trial structure was refined by the method of full-matrix least-squares to a final R index of 0·041. There are two non-equivalent azide groups, a four coordinated apparently symmetric azide and a five coordinated azide with a slight probable asymmetry. Barium atoms are surrounded by nine azides, in the form of a right triangular prism with three azides near the centers of each of the three vertical faces. The structure consists of infinite Ba–N bond chain layers, packed laterally with long Ba–N bonds. An inspection of the thermal ellipsoids suggests that the thermal vibrations of the nitrogen atoms can be described largely in terms of rigid-bar angular oscillations of the azide axis with the larger amplitude in the direction of lesser constraint.

Introduction

Barium azide $[Ba(N_3)_2]$ crystallizes in both hydrated and anhydrous forms of which the former is the easier to

grow from aqueous solution although the hydrated crystals are subject to very slow dehydration in air. The lattice parameters of $Ba(N_3)_2 \cdot H_2O$ were investigated some years ago by Günther, Porger & Rosboud (1929). The anhydrous barium azide, $Ba(N_3)_2$, was prepared and investigated for the first time in single crystal form by Torkar, Krischner & Radl, (1965). They deter-

* Guest at Army Materials and Mechanics Research Center, Watertown, Mass.

mined the lattice parameters of the monoclinic unit cell to be $a=9{\cdot}59$, $b=4{\cdot}39$, $c=5{\cdot}42$ Å, $\beta=99{\cdot}75°$, with 2 molecules per unit cell. They made similar investigations of $Ba(N_3)_2 \cdot H_2O$ and $Ba(N_3)_2 \cdot (1{\cdot}5)H_2O$.

Recently, Abel & Glen (1968) attempted to determine the structure of anhydrous barium azide by X-ray diffraction in our laboratory. They obtained the unit cell parameters: $a=9{\cdot}60$, $b=4{\cdot}40$, $c=4{\cdot}42$ Å, $\beta=99{\cdot}80°$, which essentially agree with those of the previous investigators. However their attempt to determine the structure was unsuccessful. This may be attributed to the fact that the crystal disintegrates rapidly in X-ray radiation, which results in a reduction of the intensities by as much as a factor of $\frac{1}{2}$ during an exposure of several hours.

Accordingly, the present neutron diffraction study was undertaken. No intensity changes were observed due to the neutron irradiation. The unit-cell parameters given by Torkar et al. (1965) were used for this study, assuming the standard deviations as $0{\cdot}005$ Å for the cell lengths and $0{\cdot}05°$ for the β angle.

Experimental

A flat, pillar-like, single crystal of anhydrous barium azide which was grown by Marinkas (1966) was used for this experiment. The crystal was shaped to a long cylindrical from, approximately 2 mm in diameter and 12 mm long along the unique axis (b axis), and was mounted on the goniometer cradle with the unique axis parallel to the goniometer rotation axis. The diffraction intensities were measured by ω–2θ step scanning with $0{\cdot}1°$ step interval in 2θ angle over the entire range of each reflection peak, using a conventional two-axis neutron diffractometer at the AMMRC reactor. A low efficiency transmission type monitor counter was used in the incident beam and the diffraction intensities were measured for a preset number of incident neutrons. A
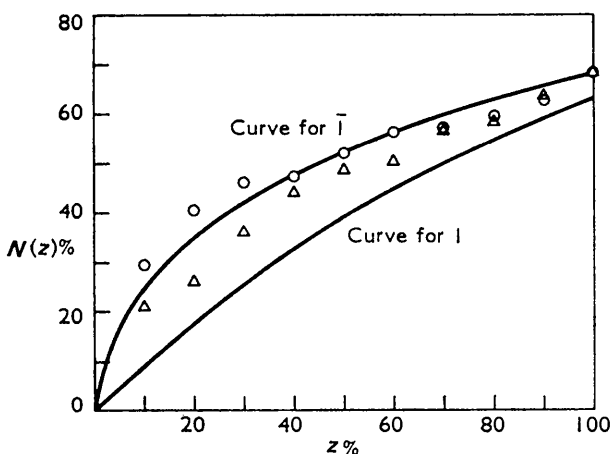

Fig. 1. $N(z)$ distribution curves for Ba(N₃)₂. Circles for [010] zone data and triangles for the combined data of [100] and [001] zone.

complete set of three-dimensional reflection data (non-overlapping) was collected within the range of 90 degrees in 2θ angle, using $0{\cdot}985$ Å wavelength neutrons. Among the 776 reflections investigated, 632 reflections showed measurable intensity. A systematic absence appeared in $0k0$ reflections for $k=2n+1$, which implies twofold screw axis symmetry around the b axis. Hence, the space group could be either $P2_1$ or $P2_1/m$.

The intensity statistics were obtained by the $N(z)$ distribution method (Howells, Phillips & Rogers, 1950) and were applied to zone data to find the correct space group from the two choices. In Fig. 1 the circles represent [010] zone data and the triangles are combined data of the [100] and [001] zones. Here, the reflections with two zero indices and the data with scattering angle less than 12 degrees were omitted. The observed intensity distributions of [010] zone data are higher than the theoretical centric distributions for low z values, and that of [100] and [001] zone data is lower. However, they terminate with $N(1{\cdot}0)=0{\cdot}68$ which agrees with the theoretical value for the centric system. Consequently, the $N(z)$ test is favorable for the centrosymmetric space group $P2_1/m$.

The observed intensities of hkl reflections were practically the same for all even numbered k (or odd numbered k) with any given h and l, except for the thermal vibration effect. In addition, the intensities of $0kl$ reflections with even number k were strongest among all the observed reflections. These facts imply that the phase angle $2\pi(hx+ky+lz)$ of the hkl reflections either remains constant or changes sign uniformly for all the atom positions (xyz) for a change in k of $\Delta k=2$. Consequently, the y-coordinates of all the atoms in a unit cell are restricted to two sets of values, $(0$ and$\frac{1}{2})$ or $(\frac{1}{4}$ and $\frac{3}{4})$. Since the crystal possesses twofold screw axis symmetry around the b axis, it becomes clear that the atoms are arranged in the centrosymmetric space group $P2_1/m$ with an inversion center at $y=\frac{1}{4}$ (or 0), of which the latter was chosen for convenience. Considering the known fact that the N–N distances within an azide group are much shorter than the distances between the two planes $(b/2=2{\cdot}195$ Å$)$, the three nitrogen atoms of an azide group must occupy the same plane. Consequently, it is further deduced that two formula-units of Ba(N₃)₂ in a unit cell must be divided equally into the two planes to form two equivalent atom layers with one molecule each. The two layer arrangement in a unit cell was further confirmed by the following Patterson synthesis.

A three-dimensional Patterson function was calculated by the use of all observed data including zero intensity reflections, as shown in Fig. 2. All the vector peaks were observed only in the two layers at $y=0$ and $\frac{1}{2}$, as expected from the previously found layer arrangement. The layer arrangement of Ba(N₃)₂ together with the known structure of the N₃ ion, which is approximately linear with equal N–N distances within an azide group, simplifies the interpretation of the Patterson function considerably. All dominant intensity peaks

form a linear pattern or a parallelogramic grid with three rows and columns equally spaced ($\sim 1 \cdot 17$ Å spacing). It is readily determined that these are the N–N peaks, and the two azide groups in each layer of the unit cell are oriented with different directions (parallel to the two sides of the parallelogram). The Ba–N peaks are also observed with weak intensity as indicated by dotted circles in the map because of its weak coherent scattering cross section which is less than $\frac{1}{3}$ of that of the N atom.

The approximate positions of all atoms were found in site (e) of the space group $P2_1/m$ (*International Tables for X-ray Crystallography*, 1952) and they were further refined by the full-matrix least-squares refinement. The initial refinement with an isotropic temperature factor for each individual atom was performed using all data including zero intensity reflections for two cycles. After applying the secondary extinction corrections for the reflections of large observed intensity, another two-cycle refinement was carried out with the non-zero intensity reflections only, which reduced the conventional R index ($R = \Sigma \ |F_o - |F_c||/\Sigma \ F_o$) to 9%. Then, anisotropic temperature factors were assigned to each atom

and the refinement was continued with two cycles, application of final secondary extinction corrections, and another two cycles. The final secondary extinction correction factors were given by exp $(6 \cdot 485 \times 10^{-6} Q)$, and it was applied uniformly for all reflection planes whose observed intensity, Q, is more than 10^4. Until this stage, all observed data were given unit weight. The discrepancy factor after the last cycle was $R = 0 \cdot 040$, $wR = (\Sigma \ w(|F_o| - |F_c|)^2/\Sigma \ w \ F_o{}^2 = 0 \cdot 042$, with the parameter shift less than $0 \cdot 01 \sigma$ for all parameters. The final three-cycle refinement was carried out by applying individual weights to all observed data based on counting statistics as described by Evans (1961). The parameter shift in the last cycle was essentially zero. The final discrepancy factor was $R = 0 \cdot 041$, $WR = 0 \cdot 039$. The final least-squares parameters are given in Table 1 with the estimated standard deviations in the parenthesis.

The refinement was based on the structure factors. The quantity minimized was $\Sigma w(|F_o| - |F_c|)^2$. A set of crystallographic programs, re-edited by Gvildys (1965), was used for the Fourier summation, the least-squares refinement, and the calculation of the interatomic distances and angles.
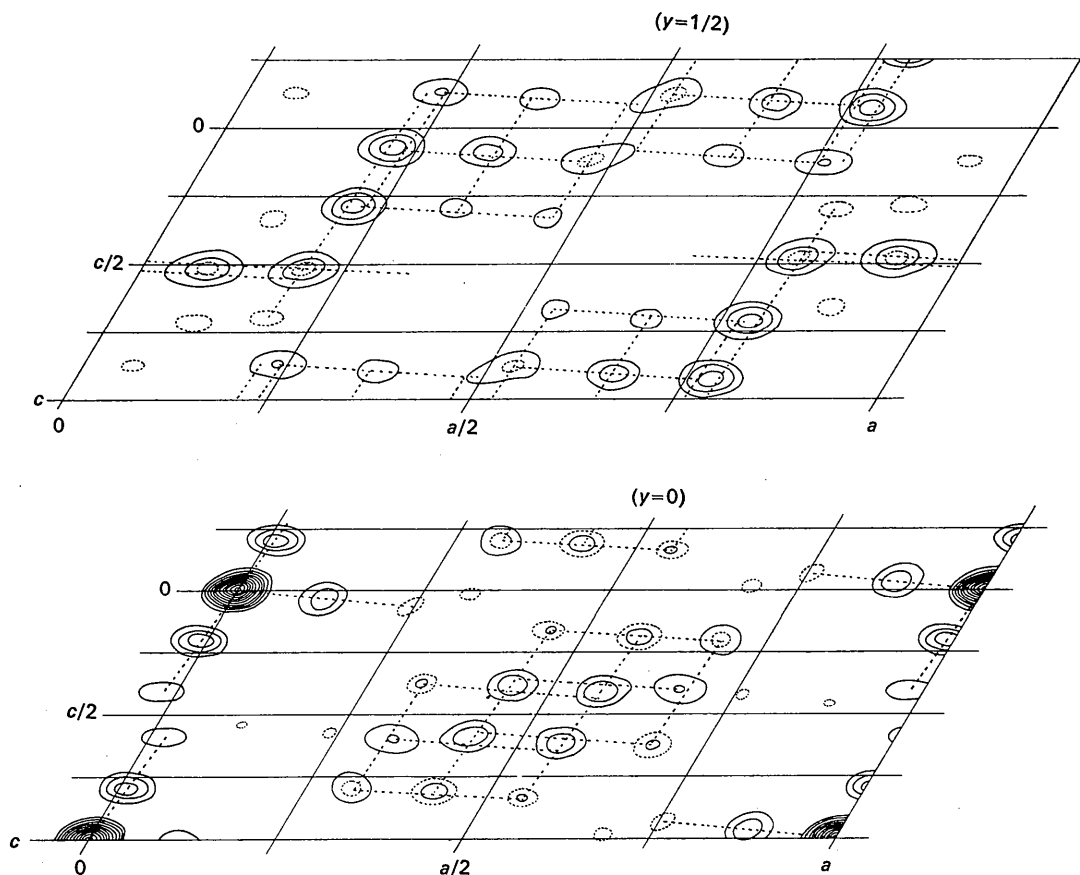

Fig. 2. Patterson function of $Ba(N_3)_2$ projected on (010). The arrangement of the N–N vector peaks shows the linear and the grid pattern as indicated with dotted lines.

Table 1. *The final least-squares parameters and their standard deviations (in parentheses)*

All values have been multiplied by 10^4. The temperature factor is of the form:

$$\exp\left[-(\beta_{11}h^2 + \beta_{22}k^2 + \beta_{33}l^2 + 2\beta_{13}hl)^*\right].$$

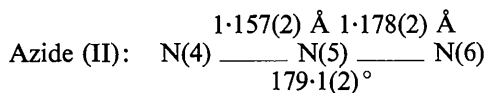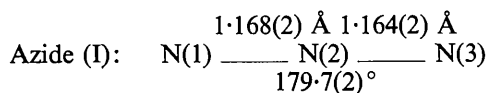|	x/a	y/b	z/c	β_{11}	β_{22}	β_{33}	β_{13}
N(1)	−825 (2)	$\frac{1}{4}$	2263 (4)	26 (2)	234 (9)	276 (7)	9 (3)
N(2)	411 (2)	$\frac{1}{4}$	2579 (3)	29 (1)	123 (6)	92 (4)	10 (2)
N(3)	1642 (2)	$\frac{1}{4}$	2904 (3)	32 (2)	288 (10)	135 (5)	11 (2)
N(4)	−3824 (2)	$\frac{1}{4}$	4383 (3)	59 (2)	139 (7)	63 (4)	25 (2)
N(5)	−3921 (2)	$\frac{1}{4}$	6483 (3)	30 (1)	98 (6)	50 (4)	9 (2)
N(6)	−4039 (2)	$\frac{1}{4}$	8611 (3)	41 (2)	157 (7)	45 (4)	10 (2)
Ba	2822 (3)	$\frac{1}{4}$	−1709 (5)	23 (2)	79 (10)	63 (7)	9 (3)

* $\beta_{12}=0$, $\beta_{23}=0$ by symmetry.

Table 2. *Observed and calculated structure factors of* Ba(N₃)₂

Unobserved reflection intensities are marked with an asterisk. (Scale factor of $F_c = 10\cdot107602$.)

Observed and calculated structure factors are given in Table 2.

Atomic arrangement

There are two molecules in a unit cell of the anhydrous barium azide crystal and all the atoms are located on the two mirror planes of the $P2_1/m$ space group. The crystallographic structure is composed of an infinite chain of Ba–N bonds which run between the barium atoms and two distinct azide groups, namely azide (I) and azide (II), as shown in Fig. 3. The azide (I) is linear and symmetric within the estimated standard deviations, but the azide (II) is probably slightly bent and probably assymmetric. Their dimensions are given as the following:

$$\text{Azide (I):} \quad \text{N(1)} \underset{179 \cdot 7(2)^\circ}{\overset{1 \cdot 168(2) \text{ Å} \quad 1 \cdot 164(2) \text{ Å}}{\rule{0.5cm}{0.4pt} \text{N(2)} \rule{0.5cm}{0.4pt}}} \text{N(3)}$$

$$\text{Azide (II):} \quad \text{N(4)} \underset{179 \cdot 1(2)^\circ}{\overset{1 \cdot 157(2) \text{ Å} \quad 1 \cdot 178(2) \text{ Å}}{\rule{0.5cm}{0.4pt} \text{N(5)} \rule{0.5cm}{0.4pt}}} \text{N(6)}$$

The azide (I) is in the mirror plane with its axis oriented 8 degrees from the crystallographic a axis and is surrounded by 4 barium atoms, 2 at each end of the azide axis. The terminal nitrogen atom, N(1), is coordinated to those Ba atoms which occupy mirror image positions in the neighboring planes. These N(1)–Ba bonds form a continuous chain running along the b axis direction. The other terminal nitrogen atom, N(3), is bonded to the two barium atoms on the same mirror plane forming a bond chain in the c-axis direction.

The azide (II) is also lying on the mirror plane with its axis oriented 5 degrees from the c-axis direction. It has five barium neighbors, among which the two in the upper plane are the mirror images of those in the lower plane, or *vice versa*. One mirror image pair of Ba atoms is bonded to the terminal nitrogen atom, N(4), and the other pair of Ba atoms to the N(6) atom at the other end of the azide group, forming two bond chains in the b axis direction. The fifth barium neighbor is located on the mirror plane and is attached to the terminal nitrogen atom N(6) with a relatively longer bond length. This fifth bond is 0·1 Å longer than the other four bonds of the azide (II), and 0·05 Å longer than those of azide (I) as given in Fig. 3. The above-discussed bond chains in the crystal are linked to each other by sharing a common barium atom and form an independent layer perpendicular to the a axis. These independent layers are then interlinked by a fifth bond of the azide (II), which explains the fact that the crystals cleave easily along the (100) plane. The packing of the azide (II) is more compact than that of the azide (I), as can be seen from the interazide distances in Fig. 4. All the atoms of the azide (II) are surrounded tightly by neighboring azide groups within a 3 Å range which is comparable with the closest approach of the van der Waals contact between adjacent azides ions for LiN_3 and $Sr(N_3)_2$.(Pringle & Noakes, 1968). On the other hand, the azide (I) is less crowded with only one terminal nitrogen atom, N(3), in close proximity to the azide (II). The inter-azide distances less than 3·4 Å are listed in Fig. 4.

The barium atom is also located in the mirror plane and surrounded by nine azide groups. Among the nine neighboring azides groups three are in the same mirror
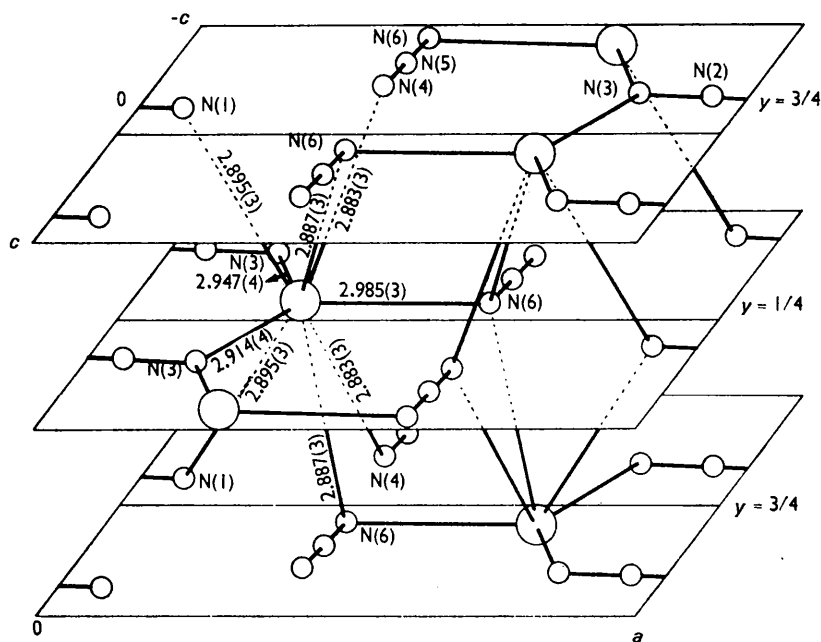

Fig. 3. Perspective view of the crystal structure of $Ba(N_3)_2$. All atoms are located on the mirror planes at $y=\frac{1}{4}$ and $y=\frac{3}{4}$.

plane and the other six are equally divided into the two adjacent mirror planes in such a way as to be related to each other by mirror reflection. Thus, the six neighbors in the adjacent layers are arranged in the form of a right triangular prism and three azide groups in the mirror plane are located beyond the centers of each of the vertical faces of the prism. A similar arrangement involving nine coordinated groups is not unusual. For example, it has been found for the nine H_2O neighbors of a Nd^{3+} ion in $Nd(BrO_3)_3 \cdot 9H_2O$ (Helmholtz, 1939). The bonds which extended from the body centered barium to the nitrogen atoms at the six corners of the prism are almost equal in length, ranging between 2·88 to 2·89 Å, as shown in the Fig. 3. The three N–Ba–N angles which face the vertical edges of the prism are also essentially the same with the value of 99°. Thus, the barium atom occupies a position very close to the exact center of the prism. The shortest Ba–Ba distance is 4·39 Å which occurs between those alligned along the b axis with a unit-cell interval.

Thermal vibrations

The anisotropic thermal vibrations for each nitrogen atom of the two azide groups were investigated as summarized in Table 3. Since the azide groups lie on the

Table 3. *The root-mean-square displacements along the principal axes of the thermal ellipsoid for each nitrogen atom of the azide group*

The estimated standard deviations of the r.m.s. displacement are given in parentheses in 0·001 Å unit.

Azide (I)					Azide (II)				
	Principal axis	r.m.s. (Å)	Angle from N(1)–N(3)	Constrained orientation		Principal axis	r.m.s. (Å)	Angle from N(4)–N(6)	Constrained orientation
N(1)	1	0·108 (3)	0·8 (1·3)	m.p.*	N(4)	1	0·088 (3)	0·8 (1·6)	m.p.
	2	0·151 (3)	90·0 (0)	b axis		2	0·117 (3)	90·0 (0)	b axis
	3	0·201 (3)	90·8 (1·3)	m.p.		3	0·164 (2)	89·2 (1·6)	m.p.
N(2)	1	0·110 (3)			N(5)	1	0·083 (3)	4·4 (3·7)	m.p.
	2	0·113 (3)	Isotropic			2	0·098 (3)	90·0 (0)	b axis
	3	0·116 (3)				3	0·117 (3)	94·4 (3·7)	m.p.
N(3)	1	0·120 (3)	5·6 (5·3)	m.p.	N(6)	1	0·080 (4)	7·8 (2·2)	m.p.
	2	0·140 (3)	95·6 (5·3)	m.p.		2	0·124 (3)	90·0 (0)	b axis
	3	0·168 (3)	90·0 (0)	b axis		3	0·136 (2)	97·8 (2·2)	m.p.

* Mirror plane.

Fig. 4. Atomic arrangement of Ba(N₃)₂ crystal projected on (010). Heavy circles for the atoms on the plane at $y = \frac{1}{4}$ and light circles for those on the plane at $y = -\frac{1}{4}$. Large circles for Ba atoms and small circles with designation number for nitrogen atoms. Short nonbonded N–N distances are given in Ångstrom units with the standard deviations less than 0·004 Å and bond angles in degree units with the standard deviations less than 0·1°.

mirror planes, the directions of the three principal axes of the vibration ellipsoids must be constrained so that one of them is directed toward the unique axis (*b* axis) direction, and other two lie on the mirror plane. For convenience, the orientations of the principal axes were described by the angle measured from the mean azide axis together with the constrained direction. The orientation of those of N(2) were not defined because its thermal vibrations are isotropic within the standard deviations of the root-mean-square displacement. Generally the thermal ellipsoid of each nitrogen in an azide group is aligned with its shortest principal axis toward the azide axis direction. The strongest vibrations of each nitrogen atom occur in the direction perpendicular to the azide axis except for the slight deviation in that of N(6). The r.m.s. displacements of the terminal nitrogen atom are always larger than those of the central nitrogen atom within an azide group. These facts suggest that there is considerable 'rigid-bar' angular oscillation of the azide axis. Similar results have been observed in the $Cu(N_3)_2$ by Söderquist (1968). The vibration directions of the terminal nitrogen atom (or angular oscillation of the azide group) are closely correlated to the nature of the azide coordination in such a way that the longest r.m.s. displacements occur in the direction of minimum constraint by the Ba–N bonds. They are the directions perpendicular to the two Ba–N bonds from each terminal nitrogen atom in the azide (I). In the azide (II), both terminal nitrogen atoms, each of which have two equally strong Ba–N bonds coupled by mirror symmetry, vibrate in the mirror plane with the longest r.m.s. component. It is also interesting to notice that the vibration amplitudes of the azide (II) are considerably smaller than those of the azide (I), which is quite reasonable in view of the fact that the arrangement of the azide (II) is much more compact than that of the azide (I) as discussed previously. The thermal vibration amplitudes of the barium metal are smallest of all with the shortest principal axis of 0·087(5) Å parallel to the *b* axis and with the longest principal axis of 0·104(4) Å on the mirror plane.

Discussion

The N–N distances in the azides of $Ba(N_3)_2$ are comparable with those in the ionic azides (*e. g.* Pringle & Noakes, 1968) or those in the symmetric azides of the heavy metal azide $\alpha\text{-}Pb(N_3)_2$ (Choi & Boutin, 1969).

The interlinking of the two independent chain layers by a long bond in $Ba(N_3)_2$ resembles that of $Cu(N_3)_2$ (Söderquist, 1968).

Single crystals of anhydrous barium azides have been irradiated at room temperature with ultraviolet radiation and the electron spin resonance spectra of N_2^- ions investigated at liquid nitrogen temperature by Marinkas & Bartram (1968). They observed lines in the e.s.r. spectra which they attributed to N_2^- ions oriented 5° from the crystallographic *c* axis (*a* axis in terms of their unit-cell notation). In addition, they suggested that the azide ion site lacks inversion symmetry on the basis of the observed hyperfine structure. Their results agree exactly with the structure of the azide (II) in the present study. The reason that the azide (I) was not observed in the e.s.r. spectra is not given in the report because the crystal structure was unknown at the time.

References

ABEL, J. E. & GLEN, G. L. (1968). Private communication.
CHOI, C. S. & BOUTIN, H. P. (1969). *Acta Cryst.* B**25**, 982.
EVANS, H. T. JR (1961). *Acta Cryst.* **14**, 689.
GÜNTHER, P., PORGER, J. & ROSBOUD, P. (1929). *Z. Phys. Chem.* B**6**, 472.
GVILDYS, J. (1965). Program B-114 (*Two- and Three-Dimensional Crystallographic Fourier Summation Program*), Program MET 153 (*A FORTRAN Crystallographic Least-squares Program*), Program B-115 (*A FORTRAN Crystallographic Function and Error Program*). Argonne National Laboratory, Argonne, Illinois.
HELMHOLTZ, L. (1939). *J. Amer. Chem. Soc.* **61**, 1544.
HOWELLS, E. R., PHILLIPS, D. C. & ROGERS, D. (1950). *Acta Cryst.* **3**, 210.
International Tables for X-ray Crystallography (1962). Vol. I. Birmingham: Kynoch Press.
MARINKAS, P. L. (1966). *Nature, Lond.* **211**, 1288.
MARINKAS, P. L. & BARTRAM, R. H. (1968). *J. Chem. Phys.* **48**, 927.
PRINGLE, G. E. & NOAKES, D. E. (1968). *Acta Cryst.* B**24**, 262.
SÖDERQUIST, R. (1968). *Acta Cryst.* B**24**, 450.
TORKAR, K., KRISCHNER, H. & RADL, H. (1965). *Monatsh. Chem.* **96**, 932.